J Soils Sediments
https://doi.org/10.1007/s11368-017-1855-5

SOILS, SEC 5 • SOIL AND LANDSCAPE ECOLOGY • RESEARCH ARTICLE

Estimation of wind and water erosion based on slope aspects in the crisscross region of the Chinese Loess Plateau

Jiaqiong Zhang[1] · **Mingyi Yang**[1] · **Xijun Sun**[2] · **Fengbao Zhang**[1]

Received: 11 June 2017 / Accepted: 13 October 2017

Abstract
Purpose The crisscross region of the Chinese Loess Plateau is affected from both wind and water erosion, and their relative contributions remain unclear. A combination analysis of ^{137}Cs inventories, surface soil sample properties, and the local wind condition allows the measurements of total soil erosion, as well as the rates of wind and water erosion that are independently affected by slope aspect at a experimental site in the study area.
Materials and methods This study selected eight straight slope for investigation. Although the slopes had similar gradients, lengths, elevations, shapes, vegetation conditions, soil types, and land-use types, they faced different aspects. This study tested the soil organic matter content, particle size, specific surface area, and ^{137}Cs inventory, including the mean ^{137}Cs reference inventory from a region of flat grassland near a century-old temple located on the top of a hillslope. Water erosion were assumed to be similar for slope aspects on condition that rainfall and environmental conditions were similar, and differences in erosion on slope aspects were mainly attributable to wind erosion. This assumption was confirmed by stepwise linear regression analysis, and wind erosion was estimated from total erosion and water erosion.
Results and discussion The east-facing slope experienced almost no wind erosion, and erosion (91.4 t ha^{-1} year^{-1}) it experienced was primarily caused by water according to estimation of total erosion and analysis to wind conditions. Based on the assumption that water erosion was similar on all slopes, the west-facing slope exhibited a similar rate of water erosion to the east slope, while the rate of wind erosion was 16.9 t ha^{-1} year^{-1}. The northwest slope had the highest wind erosion rate (42.3 t ha^{-1} year^{-1}), while the slope opposite to it (the southeast slope) had the highest wind deposition rate. Wind erosion on average contributed 27.4% to total erosion on windward slopes (northwest and north), while deposition occurred on the opposite leeward slopes (southeast and south).
Conclusions Although water erosion was found to be the primary driver of soil loss in this watershed, the effect of wind erosion cannot be neglected. It was mainly response for the erosion difference on slope aspects.

Keywords ^{137}Cs measurements · Contribution · Erosion driver · Slope aspect · Wind erosion and deposition

Responsible editor: Renduo Zhang

Electronic supplementary material The online version of this article (https://doi.org/10.1007/s11368-017-1855-5) contains supplementary material, which is available to authorized users.

✉ Mingyi Yang
ymyzly@163.com

[1] State Key Laboratory of Soil Erosion and Dryland Farming on the Loess Plateau, Institute of Soil and Water Conservation, Northwest A&F University, Yangling, Shaanxi 712100, China

[2] Xi'an Agro-technical Extension Station, Xi'an, Shaanxi 710061, China

1 Introduction

Soil is the foundation of biodiversity, ecosystem services, land degradation, energy security, food, and water supplies (Brevik et al. 2015; Keesstra et al. 2016; Wang et al. 2017). Accordingly, soil erosion is a significant threat to the capacity of ecosystem services of soil. Soil erosion is affected by multiple factors, for which terrain factors, such as slope gradient, length, shape, and aspect, are very important in hilly areas (USDA 1996; Renard et al. 2011). Although the influence of slope gradient, length, and shape has been studied in detail

Published online: 23 October 2017

(Pennock and Jong 1987; Stefano et al. 2000; Zhang et al. 2013), relatively few studies have dealt with slope aspect, even though it is considered to be the most important terrain factor after slope gradient (Carter and Ciolkosz 1991). Researchers have attributed the varying intensities of soil erosion on different slope aspects to changes in hydrological rainfall, wind-driven rainfall, solar radiation, vegetation condition, antecedent soil moisture, and parent material (Sigua and Coleman 2010; Beullens et al. 2014; Marzen et al. 2015). These erosional differences also affect soil formation, transpiration and temperature, landform evolution, the transport and distribution of nutrients and carbon, and microbial properties (Franzmeier et al. 1969; Sigua and Coleman 2010; Huang et al. 2015; Fang and Guo 2015). Previous studies related to the effects of slope aspect on soil erosion were mainly conducted in areas dominated by water erosion (Huang et al. 2015), but they did not include areas facing multiple erosion forces, such as those seen in the wind–water erosion crisscross region of China. In addition, most studies used only GIS and DEM analyses, and few were based on field measurements (Li et al. 2005).

The wind–water erosion crisscross region of China is a highly eroded belt located on the northern border of the Chinese Loess Plateau. The geographic coordinates of this region are 35° 20′–40° 10′ N, 103° 33′–113° 53′ E (see the map in Fig. 1). In other areas of the plateau, either wind or rain dominates as the primary agent of erosion, but in the crisscross region, both these forces are significant, which result in the highest erosion rates on the plateau. These forces have produced a characteristic terrain covered by a network of valleys and gullies. Moreover, eroded soil is an important source of sediments, especially coarse particles, in the lower reaches of the Yellow River (Zha et al. 1993). Erosion also ravages productive farmland and contributes to air pollution; for these reasons, understanding both wind and water erosion in the crisscross region of China is clearly of the highest economic and environmental importance.

To date, study results on the contributions of wind and water erosion in the crisscross region of China have been inconsistent. Both Dong (1998) and Zhang (1997) conducted studies in the Liudaogou watershed, but their results suggested a water-to-wind erosion ratio ranging from 4.69:1 to 12.25:1, with a mean wind erosion rate from 18.87 to 32.00 t ha^{-1} $year^{-1}$. Such inconsistent results may be due to the methods used, which treat water erosion and wind erosion as independent processes. Before recent advances in erosion measurement, wind and water erosion were measured using different techniques that did not consider the interrelations between these two processes. Researchers studied wind erosion by tracking changes in soil surfaces or analyzing particulate matter collected from the air (Offer and Goossens 1995; Hagen et al. 2010), while water erosion was typically studied by measuring sediment and runoff (Owens and Xu 2011; Zhang et al. 2011). These techniques, while they were the best available approaches at that time, are inadequate considering the complexity of the task. Furthermore, although remote sensing could be applied to assess water and wind

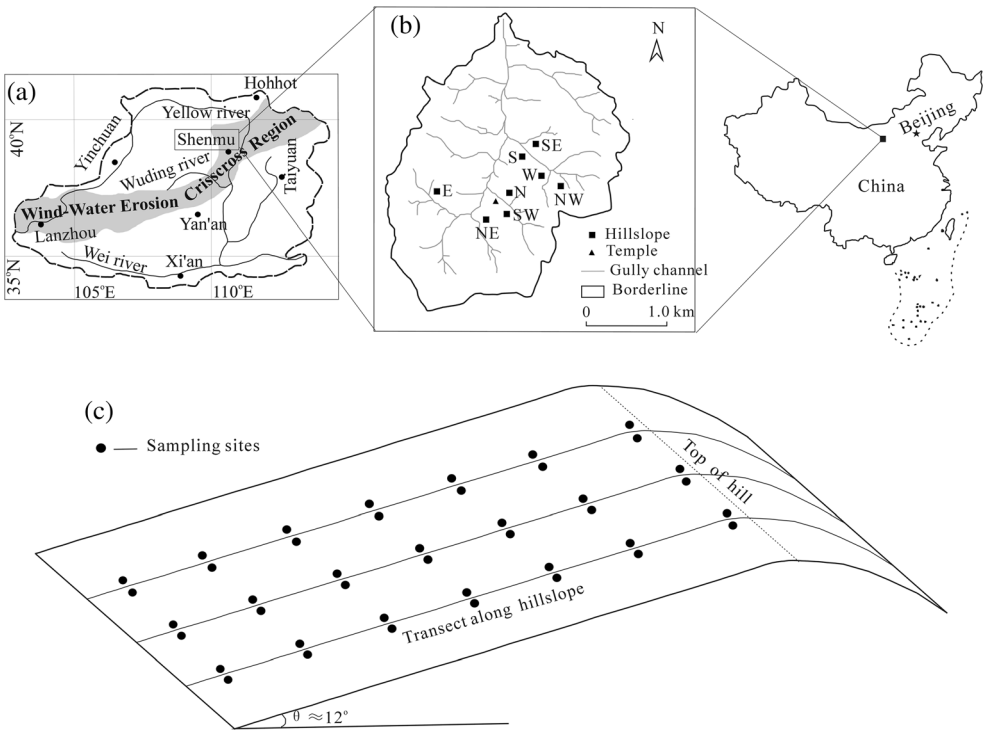

Fig. 1 Study area (**a**, **b**) and layout of soil sampling grids (**c**). **a** Crisscross region of the Loess Plateau. **b** Locations of the study sites in the Liudaogou watershed. **c** The soil sampling grid as applied to each of the eight slopes, which shows transects and sampling sites

erosion, it is not sufficiently accurate for quantitative studies (Ganasri and Rames 2016; Zhou et al. 2016).

Measurements of radionuclides could be used to study both water and wind erosion and also to comprehensively study their interactions. Cesium-137 (^{137}Cs) has been widely used in water erosion studies, and its use was extended to wind erosion studies in the 1990s (Ritchie and McHenry 1990; Sutherland et al. 1991; Yang et al. 2006; Van Pelt 2013). This method is able to overcome many problems in measuring erosion and deposition rates, and has been applied successfully in many regions of the world (Zapata et al. 2003). However, few studies have applied this technique to study both wind and water erosion within the same terrain. Li et al. (2005) used ^{137}Cs measurements on slopes facing the four cardinal directions in the Liudaogou watershed and showed that soil erosion rates on these slopes were significantly different and that wind erosion contributed greater than 18% of total erosion. Unfortunately, their results were not sufficiently detailed to quantify erosion rates on the slopes facing different directions (ordinal directions), and the contribution of wind erosion was estimated based only on the difference between south-facing and north-facing slopes.

The present study used soil fraction analyses and ^{137}Cs measurements to investigate soil loss on eight typical slopes in the Liudaogou watershed. These slopes face north (N), northeast (NE), east (E), southeast (SE), south (S), southwest (SW), west (W), and northwest (NW), but have similar slope gradients, lengths, elevations, shapes, vegetation conditions, soil types, and land-use type. The objective of this study was to estimate the contribution of water and wind erosion to total erosion under different slope aspects.

2 Materials and methods

2.1 Study area

This study describes landforms in the Liudaogou watershed, a typical area in the crisscross region of the Loess Plateau, located 14 km west of Shenmu County in Shaanxi Province, China (see Fig. 1a). The watershed has a total area of 6.89 km^2, and it is characterized by a mean gully-channel density of 7.4 km km^{-2}. Elevations range from 1273.9 m AMSL in the northwest to 1081.0 m AMSL in the southeast. The region's highly fragmented landforms are dominated by loess hills and exhibited both aeolian (i.e., wind) and fluvial (i.e., water) geomorphologic characteristics. The local weather is characterized by dramatic inter-annual variations. Weather records from 1957 through 2011 indicate an annual average temperature of 8.9 °C with a recorded maximum of 25.0 °C in July and a minimum of − 8.1 °C in January. Annual precipitation averages 422.7 mm, most of which (76.3%) falls from June through September. The prevailing wind is from the northwest, with an average velocity of 3.6 m s^{-1}, and an average of 13.5 days of gale winds (≥ 17 m s^{-1}) per year. There are also frequent episodes of blowing sand (approximately 255.1 h year^{-1}), most of which (63.0%) occur in April. Local vegetation is sparse, and slope tillage croplands are widely distributed; almost all slopes are at least in part cultivated. The lack of ground cover allows extensive water and wind erosion to occur throughout the year due to strong winds and heavy rainfall.

2.2 Soil sampling

Eight straight hill slopes in the watershed were chosen for sampling (Fig. 1b). Although these slopes were as nearly identical as possible with regard to slope gradient, length, elevation, vegetation condition, soil type, and land-use type, each slope faced a different direction (i.e., N, NE, E, SE, S, SW, W, and NW). The average gradient was approximately 12°, and the common effective sampling length was approximately 70 m, measured from the top of the hill downwards. The lower sections of slopes were not included, since the gullies or valleys at the slope bottoms varied significantly. For all slopes, in the sampling areas of all slopes, there were no visible traces of erosion or deposition by wind or rainfall. Moreover, during field observation on the NW slope in 2014, we collected 1.96 t ha^{-1} of sediment from a 20-m × l-m plot during the rainy season (total rainfall was 405.4 mm). Three soil traps (60 cm tall, 5 mm opening width with a collecting efficiency approximately 80%) located on the flat hilltops facing the NW collected few (< 145.6 g m^{-1}) particles during the windy season. In 2004 (with a total rainfall of 426.6 mm), on a SE-facing slope located south of our study area, Jiang and Shao (2011) collected 2.33 t ha^{-1} sediments from a grassland plot (20 m × 5 m) under 80% vegetative cover. These data suggested low soil erosion on slopes in the study area and that together wind erosion and water erosion removes just a thin layer of surface soil each year. Prior to 2000, all hillslopes applied in this study were cultivated land. These croplands were plowed along contour lines using an animal-drawn, triangular, single-furrow plow. The tillage depth was approximately 20 cm, and the furrow width averaged 15 cm. These slopes have since become grasslands under the "Grain for Green" program, a national conservation program initiated by the Government of China in 1999. The well-established vegetation *Stipa bungeana* (Gramineae) is the dominant species in the region, and we determined that there was similar vegetation cover (from 60.0 to 70.0%) on the eight selected slopes, using the quadrat method (1 m × 1 m in close proximity to every other sampling site along the middle transect of each slope). Total vegetation cover averaged 66.5% in October 2014 (residue cover included). Therefore, loss soil on these slopes could be due to wind, rainfall, and tillage before 2000, but only could be due to wind and rainfall

processes after 2000. The greatest distance between any sampled slope was less than 2.0 km. Thus, ^{137}Cs analysis is appropriate in this case, based on the similar conditions and the locations of the eight slopes.

The soil sampling strategy used for ^{137}Cs testing in this study was based on transects. We marked three evenly spaced transects on each slope, all of which extended from the top of the hill downwards for approximately 70 m; seven soil collection locations were spaced at equal intervals along each transect line. All soil samples were taken at a depth of from 0 to 30 cm using a steel core tube with an inner diameter of 6 cm. The uppermost sampling sites were approximately 1 m from the hilltop (Fig. 1c). Previous studies (Zhang et al. 1990, 1994; Li et al. 2005) have demonstrated that a depth of 30 cm is sufficient to detect ^{137}Cs activity for cultivated land, depending on the position of the sampling site on the slope. To increase the accuracy of our results, we collected two soil cores 0.1 m on either side of the transect line at each sampling site. These two cores were combined, giving a total of 21 samples for each slope, and tested ^{137}Cs activity separately. We also collected soil samples at depths of from 0 to 5 cm and from 40 to 45 cm along transects near each ^{137}Cs sampling sites. We took two samples from either side of each transect, making for a total of 7 surface soil samples and 7 sub-tillage samples (40–45 cm) for each slope. We collected these surface samples for analysis of grain size distribution, specific surface area (SSA), and organic matter content, to provide additional information on wind erosion in the region. Reference samples for ^{137}Cs were collected from flat grasslands near a century-old temple located close to the study slopes (Fig. 1b). Grass shorter than 5 cm on average distributed in tufts with a total coverage approximately 23%. Eleven additional soil cores were taken at depths from 0 to 30 cm at randomly chosen locations in areas approximately 10 m × 15 m, each sample was greater than 300 g, used for separate testing of ^{137}Cs activity. We collected sample using a steel core tube with an inner diameter of 6 cm in a profile with a depth-incremental of 10 cm and then bulked together. The distribution of ^{137}Cs in disturbed and undisturbed soils differed (Uğur et al. 2004; Sac and Ichedef 2015). Our study also collected a group of depth-incremental samples from 0 to 30 cm depth-incremental of 5 cm using a steel core tube with an inner diameter of 6 cm.

2.3 Soil analysis

All samples were air-dried, ground, sieved through a 1-mm screen, fully mixed, and weighed. They were analyzed at the State Key Laboratory of Soil Erosion and Dryland Farming on the Loess Plateau, Institute of Soil and Water Conservation, Chinese Academy of Science and Ministry of Water Resources during November and December 2014.

Each surface soil sample was divided into two parts: one part was passed through a 0.25-mm sieve and its soil organic matter content was measured using dichromate oxidation and external heat methods; particle size analysis was conducted on the second part, using a Mastersizer 2000 particle size analyzer (Malvern Instruments, Malvern, UK). Values of SSA were estimated from the particle size distribution, assuming spherical particles. All samples were tested twice. The grain size of particles was classified according to the United States Department of Agriculture (USDA) soil particle size classification system, and soil textures were described by the percentage of clay (< 0.002 mm), silt (0.002 to 0.05 mm), and sand (0.05 to 2 mm) (Minasny and McBratney 2001).

The content of ^{137}Cs was measured using low-background gamma spectrometry with a hyperpure coaxial germanium detector linked to a multi-channel digital analyzer system (EG and G, ORTEC). All sample weights were greater than 300 g. All ^{137}Cs samples were measured at 661.6 keV, and count times were typically over 28, 800 s. The minimum detectable activity value of the instrument was 0.2 Bq kg^{-1} in this study calculated from the equation of GB/T 11713-2015 (2015).There were 25 counting channels used in the calculation of ^{137}Cs activity. Results had a precision of approximately 6% at the 95% level of confidence.

2.4 Calculation of net soil loss

Net soil loss from each sampling location was calculated using a simplified mass balance model (Zhang et al. 1990; Walling et al. 2007). The reliability and precision of this model have been demonstrated in several sloping field soil erosion estimation applications (Yang et al. 2004; Sac et al. 2008) (the possible effects of tillage erosion are discussed in Section 4.1). The model used the following equations:

$$Y = \frac{10\mathrm{dB}}{P}\left(1-\left(1-\frac{X}{100}\right)^{1/(t-1963)}\right) \quad (1)$$

$$X = 100\frac{A_{\mathrm{ref}}-A_t}{A_{\mathrm{ref}}} \quad (2)$$

where

- Y is the mean annual soil loss (t ha^{-1} year^{-1});
- d is the depth of the plow layer (m), 0.2 m in this study;
- B is the bulk density of soil (kg m^{-3}), which was 1120 kg m^{-3};
- P is the particle size correction factor;
- X is the percentage reduction of the total ^{137}Cs inventory;
- t is the sampling year (2014);
- A_{ref} is the local reference inventory of ^{137}Cs (Bq m^{-2}), which averages 1150 ± 132 Bq m^{-2}; and
- A_t is the measured ^{137}Cs inventory at the sampling point (Bq m^{-2}).

The distribution of ^{137}Cs activity is characterized by a typical vertical depth distribution in undisturbed soil. We determined that ^{137}Cs activity decreased exponentially with increasing sampling depth (Fig. 2). Generally, ^{137}Cs is prone to be absorbed onto fine particles, and both water- and wind-driven erosion soil particles are sorted by size during transport. The particle size correction factor P is therefore necessary for estimation. In water erosion studies, the mobilized sediment is easy to collect, and its SSA can be calculated accurately. However, in the wind erosion or wind–water erosion studies, the eroded sediment is difficult to collect, and it is therefore difficult to calculate an accurate SSA of mobilized sediment. Yang et al. (2013) used the SSA of sediment remaining after erosion to calculate P, and we also applied this method in our study. The remaining soil often is coarser than the original soil; consequently, P should generally be below 1.0. The P values for slopes were calculated using Eq. (3) (Yang et al. 2013):

$$P = \left(\frac{S_e}{S_o}\right)^v \tag{3}$$

where

S_e is the specific surface area of the remaining erosion sediment ($m^2\ g^{-1}$), represented by the SSA of soil collected from 0 to 5 cm depth;

S_o is the specific surface area of the original soil ($m^2\ g^{-1}$), determined from the SSA of soil below the tillage layer (collected from 40 to 45 cm depth in this study); and

v is a constant, set to 0.75 based on the work by Yang et al. (2013).

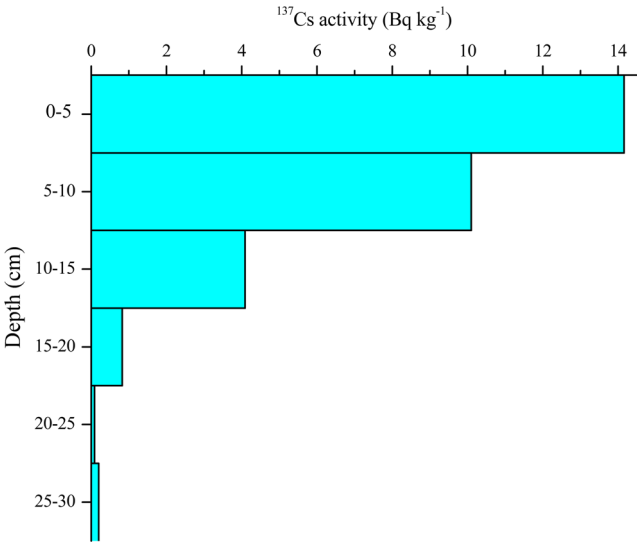

Fig. 2 The depth distribution of ^{137}Cs activity at the reference site

2.5 Discrimination of wind and water erosion

The seasonal distribution of the study area fluctuates between rainy and drought months. The duration of the rainy season lasts from June to September, and during this time, winds are relatively weak. There are occasional gales, but most are random and of short duration, typically occurring just before rainfall (Zha et al. 1993). Wind erosion is negligible during the rainy season due to high soil moisture and extensive vegetation coverage. Thunderstorms are frequent and cause intensive water erosion. The study area typically experiences a period of drought from October to May. Precipitation is scarce, and runoff and water erosion are relatively insignificant. During this period, dry weather, sparse vegetation, strong winds, and cycles of freezing and thawing tend to significantly increase wind erosion. Meteorological records of wind direction, and frequency, collected from the study area between 1961 and 2010, show that N winds had the highest average annual accumulative frequency, followed by NW and S winds, which were the second and third most common wind directions, respectively; E winds exhibited the lowest frequency (Fig. 3a). Winds that blew most frequently and forcefully during drought periods were shown to cause the greatest soil erosion, but it should be noted that not all winds led to soil erosion.

During periods of drought, winds blowing from different directions show significant differences in wind energy. Based on a 5-year study conducted from 1992 to 1996, Zhang (1997) calculated the effective wind erosion energy of different wind directions in the Liudaogou watershed. The present study used this older data set, due to a lack of relevant current observational or recorded data detailing wind speed, wind direction, and blowing hours for this region. The effective erosion energy for E winds was only 0.2 J day m^{-2}, while the greatest energy, exhibited by W winds, was 12.9 J day m^{-2} during April. Values for all other months were less than 2.0 J day m^{-2} (Fig. 3, Table S1, Electronic Supplementary Material). However, it has been suggested that the average threshold wind velocity for soil loss was 7.3 m s^{-1} in this area (Zhang 1997), indicating that when the effective erosion energy is less than 7.6 J day m^{-2}, no wind erosion will occur. Moreover, vegetation cover has increased since the implementation of the "Grain for Green" program, and the threshold wind erosion velocity should have been greater than 7.3 m s^{-1} at the time of the present study.

Soil erosion due to W winds would therefore transport only a small soil mass over the top of hills and would not produce significant deposition on the E slope. Slopes in this study were grouped into windward (NW and N) and leeward (S and SE) slopes, based on local prevailing winds. Based on the seasonal distribution of rain and drought, the effective erosion energy of winds, and the conditions of the E and W slopes, we assumed that east-facing slopes were affected primarily by water erosion, while hillsides facing the other seven directions

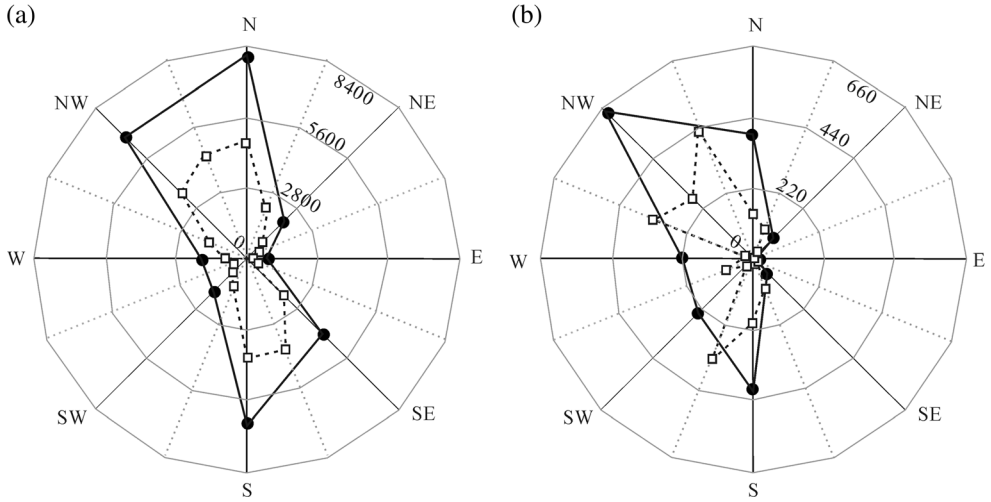

Fig. 3 Average wind direction and force in the Liudaogou watershed on 8 and 16 directions. **a** Average annual cumulative wind frequency, based on meteorological records collected from 1961 to 2015. **b** Effective wind erosion energy (J day m^{-2}) for different wind directions based on a study of Zhang (1997). Note that the original measurements for wind frequency were for 16 wind directions, which were combined into 8 directions, following the method by Zhang (1997): dividing the wind frequency of a given direction (e.g., NNW) in half and moving them to their adjacent directions (e.g., N and W). If the number was odd, it was rounded to an integer and added to the adjacent direction with a greater wind frequency; when the wind frequency of these two adjacent directions were equal, the number was added in a counterclockwise direction. The original data used in this study is shown in the Supplementary Information

underwent both water and wind erosion. The erosion on east-facing slope was used as the benchmark for estimation of the amount of wind erosion or deposition on all other slopes.

In order to confirm our assumption, linear regression analysis was applied. Factors that affects soil erosion on slopes in this study included vegetation, slope gradient and aspect, wind and rainfall conditions, and soil erodibility. We assumed that rainfall distribution on slope aspects were uniform due to the limited distance between sampling slopes (< 2.0 km) on condition that windblown rainfall was not taken into account since wind often blows just before rainfall according to a study by Zha et al. (1993). Vegetation was used its coverage due to the similarity of vegetation types. Soil erodibility was represented by the content of high erodible particles (fine sand and medium sand) according to a study by Skidmore and Powers (1982). Thus, the factors affecting variation in total erosion on slope aspects used in this study were expressed as follows: vegetation cover (%), slope gradient (°), slope aspect (°), content of fine and medium sand (%), and cumulative time of winds greater than the threshold of wind erosion ($\geq$ 7.3 m s^{-1}) based on the study of Zhang (1997). We conducted linear regression analysis using IBM SPSS 19.

3 Results

3.1 The significance of influencing factors to total soil erosion

Results from stepwise linear regression analysis showed that the cumulative time of winds greater than the threshold of wind erosion significantly contributed to the variation in total erosion on different slope aspects ($P < 0.05$, $R^2 = 0.89$) (Table 1). This confirmed our assumption that wind erosion primarily influenced variations on sloping facing different directions and also proved the emendation that water erosion was similar on the slope aspects investigated in this study.

3.2 Differences in total soil erosion rates on slope aspects

By comparing the ^{137}Cs inventory of soil samples from the eight slopes to the reference samples, we were able to calculate the overall total water and to estimate wind erosion rates for each slope based on the assumption that water erosion rates were similar on slope aspects. The NW slope, facing local prevailing winds, had the highest erosion rate (133.7 t ha^{-1} $year^{-1}$), and its opposite slope (SE) had the lowest rate, a difference of 53.1 t ha^{-1} $year^{-1}$. The N slope had the second highest erosion rate (118.9 t ha^{-1} $year^{-1}$), which was 32.0 t ha^{-1} $year^{-1}$ higher than that of the opposite (S) slope. The differences in erosion rate were similar for the remaining pairs of slopes and their opposite directions (i.e., NE–SW and E–W), with an average of 14.9 t ha^{-1} $year^{-1}$. Erosion rates of the S and E slopes were similar (< 5.2 t ha^{-1} $year^{-1}$) to those measured by Li et al. (2005), while the erosion rate on the N slope was 22.2 t ha^{-1} $year^{-1}$ higher than they reported, and W slope was much higher (96.7 t ha^{-1} $year^{-1}$) than they reported (Fig. 4a). These large differences could be related to changes in different slope gradients between these two studies. For example, the gradient of the W slope decreased downslope in the study of Li et al. (2005), while it remained almost constant in our study.

Table 1 Results of stepwise linear regression analysis

	N	NE	E	SW	S	SW	W	NW	*P* value
Slope aspect (°)	0	45	90	135	180	225	270	315	0.628
Slope gradient (°)	13.2	12.7	12.2	11.6	12.8	11.7	11.5	13	0.760
Vegetation cover (%)	60	66	68	68	69	70	68	63	0.439
Content of fine sand and medium sand (%)	39.2	32.1	36.9	41.7	41.2	56.6	39.2	32.1	0.977
Cumulative period of winds > 7.3 m s^{-1} (h)	112.8	19.2	2.4	18.1	131.6	76	55.6	152.7	0.003*

*Significant at a level of $a = 0.05$

For each slope, total erosion rate showed a slightly decreasing trend along downslope while undulating along sampling transects. The distribution of the three replication transects was roughly similar, but exhibited some changes, which could have been caused by the variation in vegetation cover and microrelief. Thus, the mean erosion rate of the three replications is reported in this study (Fig. 4b). Previous studies suggested that erosion typically increased downslope. Even a decrease in deposition can have an effect on the slope bottom if rainfall is the dominated erosion factor under the provision that surface slope condition is similar (Abrahams et al. 1991; An et al. 2014; Liu et al. 2016). Tillage leads to soil removal from upslope to downslope, and under such conditions, deposition typically occurs at the bottom of the slope. Wind erosion increases along the wind direction on the windward slope, and such changes are complex judging from research on aeolian sand dunes (Dong et al. 2014; Jiang et al. 2017). That is to say, water erosion and tillage erosion will cause an increase in erosion downslope, and variation in wind erosion is complex. Accordingly, the chaotic distribution of total erosion with obvious spatial heterogeneity should closely relate to wind erosion.

3.3 Contribution of wind and water erosion to total erosion

Conditional on the assumption of this study, erosion on the E slope was used as a benchmark to estimate wind erosion on the remaining slopes. The W slope had a wind erosion rate of 16.9 t ha^{-1} $year^{-1}$, and the erosion rate by wind on the NW and N slopes averaged 34.9 t ha^{-1} $year^{-1}$; the wind-driven erosion rate on the NW slope was higher than that on the N slope, and wind erosion contributed 31.6% of total erosion on this slope (Table 2). Moreover, the effective wind-driven erosion energy (Zhang 1997) showed that NW winds were the most erosive, although N winds were relatively strong during months when wind-driven erosion was dominate (Table S1, Electronic Supplementary Material). Therefore, both NW and N winds could cause deposition on their opposite slopes, and

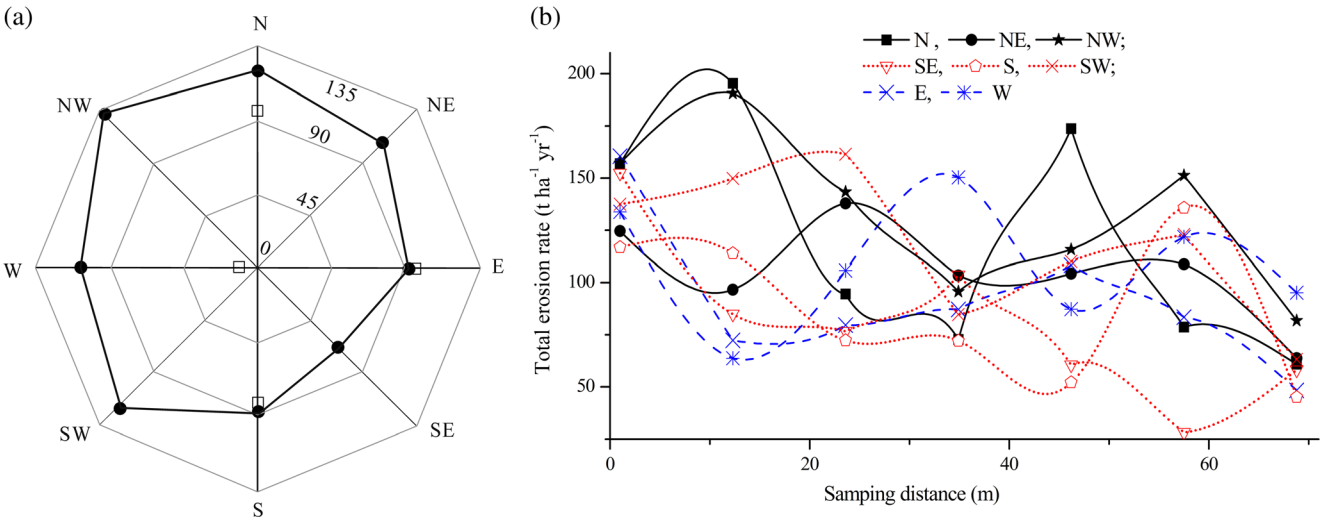

Fig. 4 Distribution of total erosion on each slope aspect ((**b**) and black circles in (**a**)) and the comparison with results from Li et al. (2005) (empty squares). In the study by Li et al. (2005), the particle size correction factor was not considered in the calculation. The slopes they investigated got steeper on downslope direction for the E (14°(average), 12–17°(range)), N (17°, 12–21°), and S (13°, 12–14°) slopes and gentler for the W (14°, 12–16°) slope

Table 2 Mean ^{137}Cs activity and soil wind erosion rate on slopes facing different directions

Slope aspect	Mean ^{137}Cs activity (Bq m^{-2})[a]	Total soil erosion rate (t ha^{-1} year^{-1})	Wind erosion/ deposition rate (t ha^{-1} year^{-1})	Percentage of wind erosion on total erosion for each slope (%)
N	173 ± 25	118.9	27.5	23.1
NE	133 ± 21	105.6	14.2	13.4
E	235 ± 27	91.4	0	0
SE	256 ± 19	80.6	− 10.8[b]	
S	208 ± 28	86.9	− 4.5[b]	
SW	160 ± 29	118.5	27.1	22.9
W	143 ± 23	108.3	16.9	15.6
NW	136 ± 23	133.7	42.3	31.6

The number for the calculation of each slope was from all 21 samples except those smaller than the minimum detectable activity of the applied gamma spectrometry. There was three for N slope, two invalid data for NW and SE slopes, and one for the remaining five slopes, respectively. In the calculation, the particle size correction factor (P) on the E slope was set to 1.0, and based on this, P for the remaining seven slopes was calculated

[a] Measurement uncertainty was at 95% confidence level. The uncertainty was calculated using its net area (A) of ^{137} Cs activity (Owens et al. 1996) as follows: $M_e = 1.96 \times 100\left(\frac{\sqrt{A}}{A}\right)$

[b] Negative values represent wind deposition

erosion estimates showed that wind deposition on SE and S slopes averaged 7.7 t ha^{-1} year^{-1}. The NE and SW slopes were not windward slopes during windy months, and the low effective wind erosion implied that the effects of prevailing winds are limited on these slopes. The contribution of wind erosion on the SW slope was 9.5% higher than that on the NE slope, mainly because the effective wind erosion energy onto the SW slope was greater. The average contribution of wind erosion to the total erosion rate on wind erosion slopes was 21.3%.

The effects of wind erosion on slope aspects are also subject to soil particle size distribution and organic matter content. Wind erosion is a process of decreases erodible particles and relative enrichment of non-erodible particles on soil surface. Although particle size shows similar effect on erodibility for both wind and water erosion, particles within a given middle size range (such as fine sand) are more susceptible to erosion, while large and very fine particles are more stable (such as coarse sand and clay). For the study region, Tang (1996) reported only negligible water erosion but strong wind erosion on almost flat (slope < 3°) hilltops. Therefore, the soil particle size distribution and organic matter content of surface soil samples from the top of each transect (1 m below the hilltops) could represent the effect of wind erosion.

Soil wind erosion typically shows strong sorting properties (Skidmore and Powers 1982). Soil samples from the NW slope had the largest fraction of coarse particles (i.e., sand) and the lowest fine particles (i.e., silt and clay), while the S slope exhibited the opposite distribution pattern. Comparing slopes facing opposite directions (i.e., N–S, E–W, NE–SW, and NW–SE), differences in sand content at the uppermost sampling sites were greatest (22.9%) between the NW and SE slopes and smallest (4.3%) between the W and E slopes. The N and NE slopes were more similar than the S and SW slopes (Fig. 5a, b). The differences in soil particle size distribution on the eight slopes represented the differences effects of wind erosion. The directions exposed to prevailing winds underwent significant erosion, while directions protected from the winds experienced little or no erosion. Sand was the primary component of surface soil samples on the NW-facing slope, which showed the most significant drop in silt content, while silt was the primary component on the remaining seven slopes. These results indicated two possibilities: (1) that sand is less likely than silt and clay to be redistributed by wind and (2) that silt in the soil is easily lost to wind erosion and can be transported long distances.

Soil organic matter binds strongly to fine soil particles, which is less likely to be lost due to wind erosion (Spain 1990). Samples from slopes facing NE, E, SE, and S contained more organic matter than the slopes facing the opposite directions (i.e., SW, W, NW, and N). We found that organic matter content was greatest on the SE slope and smallest on the NW slope (with a difference of 0.78%). Organic matter content was most similar between the NE and SW slopes (with a difference of 0.06%). The difference between the S and N slopes was 0.3%, which was greater than that between the E and W slopes (0.2%) (Fig. 5d). Despite minor variations, the general trend was clear: fine particles, including organic matter, tended to erode from slopes facing prevailing winds, leaving a more significant proportion of sand in their place. The effect of wind erosion was most prevalent on the NW direction, and silt had the highest eroded fraction compared to sand and clay. The low content of organic matter observed from the NW aspect indicated that organic matter is likely to attach more to silt particles. Thus, the loss of silt directly leads to the decrease in organic matter (Fig. 5).

Although both ^{137}Cs measurements and distributions of particle size and organic matter content imply different contributions of wind erosion on different slope aspects, it is clear from the relative proportions of eroded terrain by means of wind and water that water erosion is the primary cause of soil loss in this watershed. Typical water-eroded gullies and channels cover 32.7% of the watershed, with a density of 7.4 m km^{-2} (Zhang 1997) (Fig. 6a). Although water erosion is certainly the primary process of the landscape formation in the studied watershed, the effects of wind erosion are also significant, with aeolian landforms represented by sand sheets totaling 12.1% of the watershed (Wang et al. 1993; Zhang 1997) (Fig. 6b). Wind erosion also plays an important role in the formation of hyperconcentrated flows (i.e., sediment-saturated flows that can be classified as either fluvial or debris

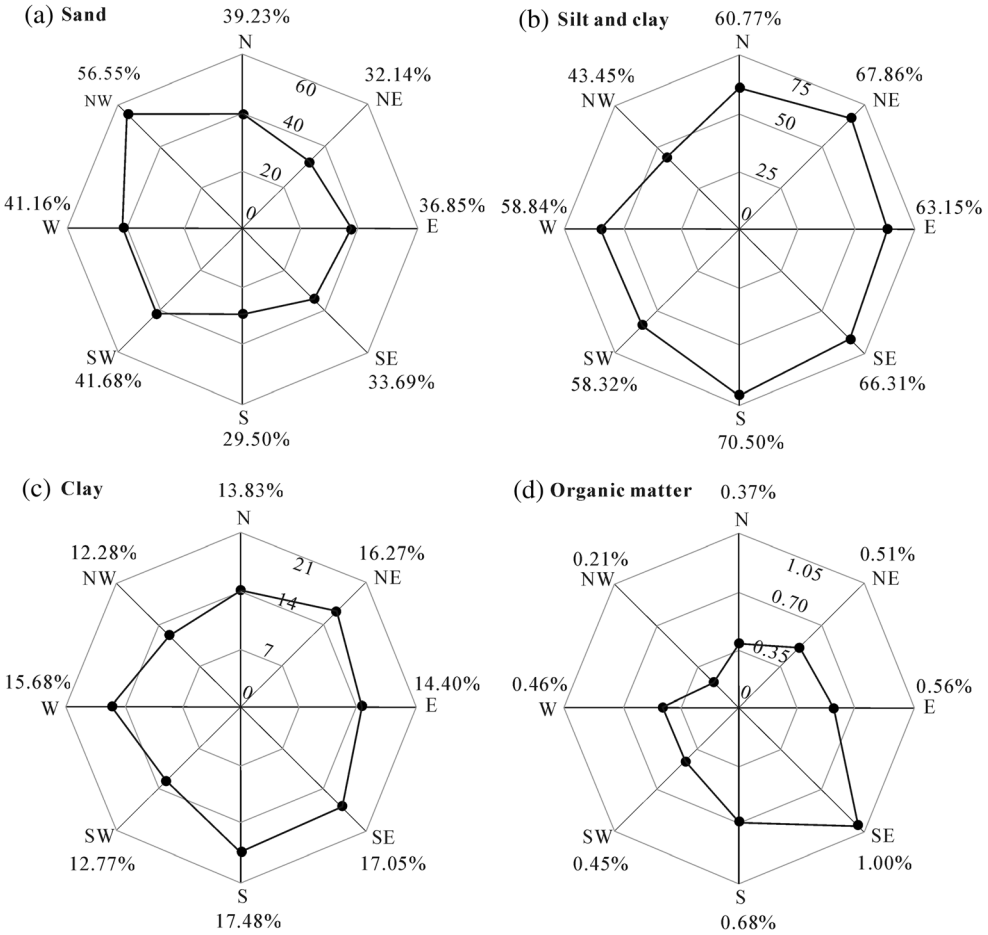

Fig. 5 **a**–**d** Percentages of soil particles (sand, silt and clay, and clay) and organic matter found in surface soil samples

flows) in the Yellow River and its tributaries (Xu 2000). Based on the assumption, in the sampled area of each slope, wind erosion rates were found to be significantly higher than deposition rates. Average soil erosion by wind exceeded 25.6 t ha^{-1} $year^{-1}$, while deposition averaged slightly more than 7.7 t ha^{-1} $year^{-1}$. In addition, results from the uppermost sampling sites indicated that the greater proportion of hilltop soil (46.2%) consisted of silt that is highly susceptible to wind erosion. Winds carry particles E and SE, whereby they contribute to river sedimentation and air pollution.

4 Discussion

4.1 Contribution of tillage erosion to total erosion

As described in Section 2.2, the eight slopes investigated in this study were croplands prior to 2000 and had been plowed once per year for an indeterminate number of years after cultivation Therefore, it is reasonable to surmise that soil erosion on sloping croplands prior to 2000 was caused by a combination of rainfall, wind, and tillage and that some portion (perhaps a significant portion) of soil loss on these slopes could have been caused by tillage erosion.

De Alba et al. (2004) and Wang (2002) suggested that tillage erosion is affected by topography and that slopes with a fairly constant gradient show significantly less soil loss than slopes with a profile curvature (i.e., convex). Soil loss due to tillage on continuously cultivated slopes, with the exception of the very top and bottom of slopes, could be ignored because soil that moves downslope from any point could be compensated for by soil washing in from upslope (Vieira and Dabney 2009). Agricultural practices in the study watershed included contour tillage with an effective width of approximately 15 cm for each tillage pass. Soil samples from the highest-elevations on the selected eight straight slopes were all taken approximately 1 m downslope from the top of the hill, a distance greater by a factor of 6 compared to the effective width of one tillage pass. Plowing would cause little net soil loss, and minor variations in hill profiles (i.e., concave and convex areas) would have also canceled each other out as well. The only net gain would have been at the bottom of the slope, below the last furrow and certainly below the proposed 70 m transects. Therefore, there would have been little or no net soil loss caused by tillage prior to 2000 on the portions of the

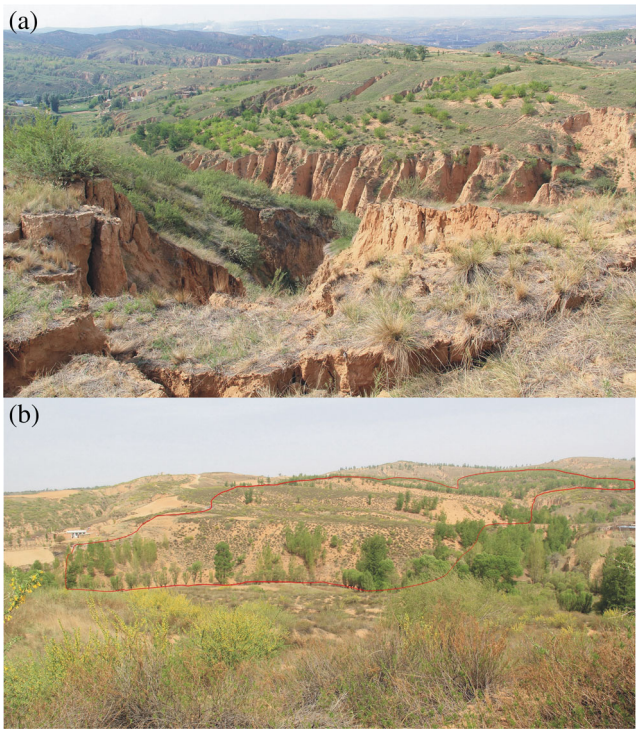

Fig. 6 Autogenetic landforms, which were primarily sculptured by water erosion (**a**) and wind erosion (**b**), seen in the red line of (**b**) was covered by sand

slopes sampled, and soil loss was therefore essentially due entirely to water and wind erosion.

4.2 Possible causes of uncertainty in this study

Two factors introduced uncertainty in this study. The first is due to surface variation on slope aspects caused by differences arising from wind-driven rainfall, solar radiation, and antecedent soil moisture (Beullens et al. 2014; Marzen et al. 2015). Using erosion on the E slope as a benchmark to estimate wind erosion on the remaining slopes, we determined that wind erosion on windward slopes (NW and N) was underestimated and that on the opposite leeward slopes (SE and S) was overestimated as a result. Compared to E slope, windward slope surfaces were more sensitive to wind during windy months, as they faced strong winds that resulted in low solar radiation and antecedent soil moisture. During rainy months, especially July and August, where the possibility of very high water erosion is a factor (high effective water erosion energy) (Table S2, Electronic Supplementary Material), prevailing SW winds drive erosive, wind-driven rainfall onto SW slope. Therefore, water erosion on SW slope should be greater than 91.4 t ha^{-1} $year^{-1}$. The second source of uncertainty is due to the use of soil erosion estimation models in conjunction with ^{137}Cs measurements. The estimation models used in this study were designed for tillage fields, while the slopes used in this study have not been plowed since 2000. This results in bias in total erosion estimates, but there is at present no better option. Nevertheless, we believe our estimation results are acceptable, since these abandoned slope farmlands are densely covered with grass and have experienced little wind or water erosion since that time. We presumed that erosion had mainly occurred during the many years of active cultivation. The 20 m × 5 m observation plots studied by Jiang and Shao (2011) in 2004 collected only 2.33 t ha^{-1} sediments from a 30-cm tall grassland under 80% vegetation cover, demonstrating limited erosion of soils under dense grassland cover. Estimation models and methods using ^{137}Cs measurements should be improved upon to make them more suitable for areas undergoing land-use changes.

5 Conclusions

Measurements of ^{137}Cs allowed for the calculation of total soil erosion caused by wind and water. Water erosion should have affected E and W slopes almost equally, because the slope gradients, lengths, elevations, shapes, vegetation conditions, soil types, and land-use types of the slopes in the study area were all similar, and no wind erosion occurred on the E slope, based on analysis of wind conditions. The assumption was validated using stepwise linear regression analysis. It showed the acceptability of the assumption and the importance of wind erosion on variation in total erosion on slope aspects. The effect of wind erosion was also indicated by the chaotic distribution of erosion rates for each slope. Given this assumption, total erosion on the E slope was considered to be caused by water erosion alone, and the amount of wind erosion was calculated from the total values and the water erosion values for the remaining seven slopes. The S and SE slopes exhibited soil deposition, while the other five slopes exhibited wind erosion. The average soil loss by wind was 25.6 t ha^{-1} $year^{-1}$ and contributed, on an average, 21.3% of the total erosion; windward slopes (NW and N) contributed 27.4%, while the deposition rate on their opposite (SE and S) slopes was 7.7 t ha^{-1} $year^{-1}$. The NW slope experienced the severest wind erosion (42.3 t ha^{-1} $year^{-1}$), and its opposite slope (SE) had the greatest amount of deposition (10.8 t ha^{-1} $year^{-1}$). This was also confirmed by the distribution of particle fraction and the content of organic matter. Therefore, water erosion must be considered to be the primary process of soil loss in this watershed, which was also confirmed by the proportion of typical terrains that were primarily formed by wind erosion and water erosion. Assuming that water erosion is in a similar range on all slopes, we can conclude that wind erosion was only a secondary process of erosion. According to the results of the regression analysis, wind was the main factor responsible for the variation in the erosion rate on slope aspects.

Acknowledgements This study was financially supported by the National Natural Science Foundation of China (Grant Nos. 41401314 and 41171228) and the Research Startup Foundation for Talents of Northwest A&F University of China (Grant No. 2013BSJJ092). We would like to express our sincere gratitude to Mrs. Li Yaqi and Mr. Xue Kai for their assistance in processing soil samples. Warm thanks are also extended to Professor Zhanli Wang for his valuable suggestions in the analysis of tillage erosion, as well as two anonymous reviewers and the editor for their valuable comments. Lastly, we would like to thank Mrs. Karen Lofstrom, Mr. Brain Doonan, and Editage for language editing.

References

Abrahams AD, Parsons AJ, Luk SH (1991) The effect of spatial variability in overland flow on the downslope pattern of soil loss on a semiarid hillslope, southern Arizona. Catena 18(3–4):255–270

An J, Zheng FL, Wang B (2014) Using ^{137}Cs technique to investigate the spatial distribution of erosion and deposition regimes for a small catchment in the black soil region, Northeast China. Catena 123: 243–251

Beullens J, de Velde DV, Nyssen J (2014) Impact of slope aspect on hydrological rainfall and on the magnitude of rill erosion in Belgium and northern France. Catena 114:129–139

Brevik EC, Cerdà A, Mataix-Solera J, Pereg L, Quinton JN, Six J, Van Oost K (2015) The interdisciplinary nature of soil. Soil 1:117–129

Carter BJ, Ciolkosz EJ (1991) Slope gradient and aspect effects on soils developed from sandstone in Pennsylvania. Geoderma 49:199–213

De Alba S, Lindstrom M, Schumacher TE, Malo DD (2004) Soil landscape evolution due to soil redistribution by tillage: a new conceptual model of soil catena evolution in agricultural landscapes. Catena 58:77–100

Dong ZB (1998) Establishing statistic model of wind erosion on small watershed basis. Bull Soil Water Conserv 18:55–62 **(in Chinese)**

Dong ZB, Lv P, Zhang ZC, JF L (2014) Aeolian transport over a developing transverse dune. J Arid Land 6(3):243–254

Fang HY, Guo M (2015) Aspect-induced differences in soil erosion intensity in a gullied hilly region on the Chinese Loess Plateau. Environ Earth Sci 74:5677–5685

Franzmeier DP, Pedersen EJ, Longwell TJ, Byrne JG, Losche CK (1969) Properties of some soils in the Cumberland Plateau as related to slope aspect and position. Soil Sci Soc Am 33(5):755–761

Ganasri BP, Rames H (2016) Assessment of soil erosion by RUSLE model using remote sensing and GIS—a case study of Nethravathi Basin. Geosci Front 7(6):953–961

Hagen LJ, Van Pelt S, Sharratt B (2010) Estimating the saltation and suspension components from field wind erosion. Aeolian Res 1(3–4):147–153

Huang Y, Liu D, An SS (2015) Effects of slope aspect on soil nitrogen and microbial properties in the Chinese Loess region. Catena 125: 135–145

Jiang N, Shao MA (2011) Characteristics of soil and water loss of different slope land uses in small watershed on the Loess Plateau. Trans CSAE 27(6):36–41 **(in Chinese)**

Jiang H, Dun HC, Tong D, Huang N (2017) Sand transportation and reverse patterns over leeward face of sand dune. Geomorphology 283:41–47

Keesstra SD, Bouma J, Wallinga J, Tittonell P, Smith P, Cerdà A, Montanarella L, Quinton JN, Pachepsky Y, van der Putten WH, Bardgett RD, Moolenaar S, Mol G, Jansen B, Fresco LO (2016) The significance of soils and soil science towards realization of the United Nations Sustainable Development Goals. Soil 2:111–128

Li M, Li ZB, Liu PL, Yao WY (2005) Using cesium-137 technique to study the characteristics of different aspect of soil erosion in the wind-water erosion crisscross region on Loess Plateau of China. Appl Radiat Isot 62:109–113

Liu Z, Yang MY, Zhang JQ (2016) Spatial distribution pattern of soil-wind erosion on slope farmlands in the wind-water erosion crisscross region of the Loess Plateau, China. Chin Sci Bull 61(4–5): 511–517 **(in Chinese)**

Marzen M, Iserloh T, Casper MC, Ries JB (2015) Quantification of particle detachment by rain splash and wind-driven rain splash. Catena 127:135–141

Minasny B, McBratney AB (2001) The Australian soil texture boomerang: a comparison of the Australian and USDA/FAO soil particle size classification systems. Aust J Soil Res 39(6):1443–1451

National Institute for Radiological Protection, China, Hainan Center for Disease Control and Prevention, School of Public Health Jilin University (2015) General analytical methods of high-purity germanium gamma spectrometer (GB/T 11713-2015)

Offer ZY, Goossens D (1995) Wind tunnel experiments and field measurements of aeolian dust deposition on conical hills. Geomorphology 14(1):43–56

Owens PN, Xu ZH (2011) Recent advances and future directions in soils and sediments research. J Soils Sediments 11:875–888

Owens PN, Walling DE, He QP (1996) The behaviour of bomb-derived caesium-137 fallout in catchment soils. J Environ Radioact 32(3): 169–191

Pennock DJ, Jong DE (1987) The influence of slope curvature on soil erosion and deposition in hummock terrain. Soil Sci 144(3):209

Renard KG, Yoder DC, Lightle DT, Dabney SM (2011) Universal soil loss equation and revised universal soil loss equation. In: Morgen RPC, Nearing MA (eds) Handbook of erosion modelling. Blackwell Publishing Ltd., Hoboken, pp 137–167

Ritchie J, McHenry JR (1990) Application of radioactive fallout cesium-137 for measuring soil erosion and sediment accumulation rates and patterns: a review. J Environ Qual 19:215–233

Sac MM, Ichedef M (2015) Application of ^{137}Cs technique for evaluation of erosion and deposition rates within cultivated fields of Salihli region. Turkey, Western

Sac MM, Yumurtaci E, Yener G, Uğur A, Özden B, Camgöz B (2008) Soil erosion determinations using ^{137}Cs technique in the agricultural regions of Gediz Basin, Western Turkey. Environ Geol 55(3):477–483

Sigua GC, Coleman SW (2010) Spatial distribution of soil carbon in pastures with cow-calf operation: effects of slope aspect and slope position. J Soils Sediments 10(2):240–247

Skidmore EL, Powers DH (1982) Soil aggregate stability energy-based index. Soil Sci Soc Am J 46:1274–1279

Spain AV (1990) Influence of environmental conditions and some soil chemical properties on the carbon and nitrogen contents of some tropical Australian soils. Aust J Soil Res 28(6):825–839

Stefano CD, Ferro V, Porto P, Tusa G (2000) Slope curvature influence on soil erosion and deposition processes. Water Resour Res 36(2):607–617

Sutherland RA, Kowalchuk T, de Jong E (1991) Cesium-137 estimates of sediment redistribution by wind. Soil Sci 151:387–396

Tang KL (1996) Discussion on comprehensive control of small watershed in water and wind crisscrossed erosion region on the Loess Plateau. Res Soil Water Conserv 3:46–55 **(in Chinese)**

Uğur A, Saç MM, Yener G, Altınbaş Ü, Kurucu Y, Bolca M, Özden B (2004) Vertical distribution of the natural and artificial radionuclides in different soil profiles to investigate soil erosion. J Radioanal Nucl Ch 259(2):265–270

USDA (1996) Wind Erosion Prediction System (WEPS) technical documentation. United States Department of Agriculture, Agricultural Research Service, Wind Erosion Research Unit, Manhattan, Kansas

Van Pelt RS (2013) Use of anthropogenic radioisotopes to estimate rates of soil redistribution by wind I: historic use of ^{137}Cs. Aeolian Res 9: 89–102

Vieira DA, Dabney SM (2009) Modeling landscape evolution due to tillage: model development. Trans ASABE 52(2):1505–1521

Walling DE, Zhang Y, He Q (2007) Models for converting measurements of environmental radionuclide inventories (^{137}Cs, excess ^{210}Pb, and ^{7}Be) to estimates of soil erosion and deposition rates. Department of Geography, University of Exeter

Wang ZL (2002) Study of tillage erosion and its effects on loess sloping land. Dissertation, Northwest A&F Univerisy **(in Chinese)**

Wang BK, Tang KL, Zhang KL, Zhang PC (1993) Types and intensity of soil erosion and its temporal and spatial distribution in Liudaogou watershed Shenmu county. In: Memoir of Northwest Institute of Soil and Water Conservation, Academia Sinica and Ministry of Water Resources 18, pp 57–66 **(in Chinese)**

Wang XM, Lang LL, Hua T, Li H, Zhang CX, Ma WY (2017) Effects of aeolian processes on soil nutrient loss in the Gonghe Basin, Qinghai–Tibet Plateau: an experimental study. J Soils Sediments. https://doi.org/10.1007/s11368-017-1734-0

Xu JX (2000) Grain-size characteristics of suspended sediment in the Yellow River, China. Catena 38:243–263

Yang MY, Liu PL, Li LQ (2004) Precision comparison of the erosion rates derived from ^{137}Cs measurements models with predictions based on empirical relationship. Acta Agric Nucl Sin 18(5):385–389 **(in Chinese)**

Yang MY, Tian JL, Liu PL (2006) Investigating the spatial distribution of soil erosion and deposition in a small catchment on the Loess Plateau of China, using ^{137}Cs. Soil Tillage Res 87:186–193

Yang MY, Walling DE, Sun XJ, Zhang FB, Zhang B (2013) A wind tunnel experiment to explore the feasibility of using beryllium-7 measurements to estimate soil loss by wind erosion. Geochim Cosmochim Acta 114:81–93

Zapata F, Garcia-AgudoE RJC, Appleby PG (2003) Handbook for the assessment of soil erosion and sedimentation using environmental radionuclides. Kluwer Academic Publishers, Dordrecht, Boston

Zha X, Wang BK, Tang KL (1993) The environment background and administration way of wind-water erosion crisscross region and Shenmu experimental area on the Loess Plateau. In: Liu YM, Wang JW, Liu Y (eds) Memoir of Northwest Institute of Soil and Water Conservation, vol 18. Academia Sinica and Ministry of Water Resources, Beijing, pp 67–74 **(in Chinese)**

Zhang PC (1997) Spatial and temporal variability of erosion by water and wind in wind-water erosion crisscross region-a case study of Liudaogou watershed in Jin-Shan-Meng contiguous areas. Dissertation, Institute of Soil and Water Conservation, China Acdemy of Scinences and Ministry of Water Resources (in Chinese)

Zhang XB, Higgitt DL, Walling DE (1990) A preliminary assessment of the potential for using caesium-137 to estimate rate of soil erosion in the Loess of China. Hydrol Sci J 35(3):243–252

Zhang XB, Quine TA, Walling DE, Li Z (1994) Application of the caesium-137 technique in a study of soil erosion on gully slopes in a Yuan area of the Loess Plateau near Xifeng, Gansu Province, China. Geogr Ann A 76(1–2):103–120

Zhang YG, Nearing MA, Liu BY, Van Pelt RS, Stone JJ, Wei H, Scott RL (2011) Comparative rates of wind versus water erosion from a small semiarid watershed in southern Arizona, USA. Aeolian Res 3:197–204

Zhang FB, Wang ZL, Yang MY (2013) Validating and improving interrill erosion equations. PLoS One 9(2):1–11

Zhou Y, Guo B, Wang SX, Tao HP, Liu WL, Yang G, Zhu JF (2016) Dynamic monitoring of soil wind erosion in Inner Mongolia of China during 1985–2011 based on geographic information system and remote sensing. Nat Hazards 83(1):1–17